Contents lists available at ScienceDirect

BBA - Molecular and Cell Biology of Lipids

journal homepage: www.elsevier.com/locate/bbalip

# 4-Hydroxynonenal induces Cx46 hemichannel inhibition through its carbonylation

Mauricio A. Retamal[a,b,*], Mariana C. Fiori[c], Ainoa Fernandez-Olivares[a,b], Sergio Linsambarth[d], Francisca Peña[d], Daisy Quintana[d], Jimmy Stehberg[d], Guillermo A. Altenberg[c]

[a] Universidad del Desarrollo, Centro de Fisiología Celular e Integrativa, Facultad de Medicina Clínica Alemana, Santiago, Chile
[b] Universidad del Desarrollo, Programa de Comunicación Celular en Cáncer, Facultad de Medicina Clínica Alemana, Santiago, Chile
[c] Department of Cell Physiology and Molecular Biophysics, Center for Membrane Protein Research, Texas Tech University Health Sciences Center, Lubbock, TX 79430-6551, USA
[d] Laboratorio de Neurobiología, Instituto de Ciencias Biomédicas, Facultad de Medicina y Facultad de Ciencias de la vida, Universidad Andres Bello, Santiago, Chile

ARTICLE INFO

*Keywords:*
Carbonylation
Cataract
Connexin
Lipid peroxide
Post-translational modification

ABSTRACT

Hemichannels formed by connexins mediate the exchange of ions and signaling molecules between the cytoplasm and the extracellular *milieu*. Under physiological conditions hemichannels have a low open probability, but in certain pathologies their open probability increases, which can result in cell damage. Pathological conditions are characterized by the production of a number of proinflammatory molecules, including 4-hydroxynonenal (4-HNE), one of the most common lipid peroxides produced in response to inflammation and oxidative stress. The aim of this work was to evaluate whether 4-HNE modulates the activity of Cx46 hemichannels. We found that 4-HNE (100 μM) reduced the rate of 4′,6-diamino-2-fenilindol (DAPI) uptake through hemichannels formed by recombinant human Cx46 fused to green fluorescent protein, an inhibition that was reversed partially by 10 mM dithiothreitol. Immunoblot analysis showed that the recombinant Cx46 expressed in HeLa cells becomes carbonylated after exposure to 4-HNE, and that 10 mM dithiothreitol reduced its carbonylation. We also found that Cx46 was carbonylated by 4-HNE in the lens of a selenite-induced cataract animal model. The exposure to 100 μM 4-HNE decreased hemichannel currents formed by recombinant rat Cx46 in *Xenopus laevis* oocytes. This inhibition also occurred in a mutant expressing only the extracellular loop cysteines, suggesting that other Cys are not responsible for the hemichannel inhibition by carbonylation. This work demonstrates for the first time that Cx46 is post-translationally modified by a lipid peroxide and that this modification reduces Cx46 hemichannel activity.

## 1. Introduction

Intercellular communication is fundamental for normal cell function, tissue coordination, and organ function. This important task is accomplished by the release of signaling molecules, and direct cell-cell contacts. Connexins (Cx) are membrane proteins that participate in both types of communication through the formation of hemichannels and gap-junction channels (GJCs). Hemichannels are formed by six Cx subunits [1] and GJCs are assembled by docking of two hemichannels, each one from a different cell [2]. Free, undocked hemichannels at the plasma membrane allow for the exchange of signaling molecules between the cytoplasm and the extracellular milieu [1], whereas GJCs mediate passive flow of ions and molecules such as second messengers between the cytoplasm of adjacent cells [1,2]. Chemical and electrical coupling through GJCs can convert neighboring cells into a coordinated functional syncytium, which is essential for the function of tissues and organs [2,3]. *In vitro* under near-physiological conditions hemichannels show a low open probability [1,4], which is nevertheless sufficient to allow the release of molecules such as gliotransmitters in astrocytes [5–7]. Accordingly, studies *in vivo* suggested relevant roles for hemichannels in brain function, including a critical role in fear memory formation [8]. Under pathological conditions where levels of inflammatory and oxidative mediators are high, there is increased hemichannel activity that can result in cell malfunctioning or even cell

*Abbreviations:* Cx, connexin; DTT, dithiothreitol; GJCs, gap-junction channels; GFP, green fluorescent protein; 4-HNE, 4-hydroxynonenal; MTSES, sodium (2-sulfonatoethyl) methanethiosulfonate; PUFAs, polyunsaturated fatty acids

* Corresponding author at: Centro de Fisiología Celular e Integrativa, Facultad de Medicina, Clínica Alemana Universidad del Desarrollo, Av. Las Condes 12438, Lo Barnechea, Santiago, Chile.
*E-mail address:* mretamal@udd.cl (M.A. Retamal).

https://doi.org/10.1016/j.bbalip.2020.158705
Received 9 March 2020; Accepted 28 March 2020
Available online 31 March 2020
1388-1981/ 

death [1,9–11]. Thus, it is critical to understand the molecular mechanisms associated to hemichannel gating under physiological and pathological conditions.

Lipid peroxides are among the molecules produced by tissues under inflammatory conditions [12,13]. These lipids are produced by enzymatic or non-enzymatic oxidation of polyunsaturated fatty acids (PUFAs) [14], and 4-hydroxynonenal (4-HNE) is one of the most common lipid peroxides produced in response to inflammation and oxidative stress [14–18]. Under physiological conditions the concentration of free 4-HNE in plasma is in the 0.3–0.7 μM range, but it can reach values 10-fold higher under oxidative conditions inside the cells [15,17]. The 4-HNE exerts many different effects through protein carbonylation, a post-translational modification [15,19,20]. As many other oxidized lipid products, it reacts with nucleophilic amino acids such as Cys, Lys and His [21], with a Cys > His > Lys preference [15]. The reversal of Cys lipid peroxidation by reducing agents such as dithiothreitol (DTT) [21–24] suggests that the modification is a dynamic process that can be modulated by the cellular redox status [17,25].

Hemichannels are affected by several molecules produced under inflammatory conditions [26–29]. Recently, the PUFAs linoleic acid and arachidonic acid have been proposed as hemichannel regulators because they reduce Cx46 hemichannel currents [30,31]. The mechanism is not well understood, but it is possible that lipid peroxides derived from oxidation of PUFAs, rather than PUFAs themselves, are the responsible molecules for their effect. Previous studies have shown that Cx26- and Cx43-GJCs are modulated by lipid peroxide-mediated pathways [32,33], but no information is available regarding the effect of lipid peroxides on hemichannels, which can display regulation and inhibition distinct from that of GJCs [31,34]. There is, however, limited evidence suggesting that lipid peroxides could modulate Cx46 hemichannel activity [35]. Here, we found that 4-HNE inhibits recombinant hemichannels formed by Cx46 in HeLa cells and in *Xenopus laevis* oocytes, and that the hemichannel inhibition seems to be associated to the carbonylation of Cx46 Cys residues. This work demonstrates for the first time that Cx46 is post-translationally modified by a lipid peroxide and supports the hypothesis that Cx46 hemichannels are sensitive to molecules associated to changes in redox potential.

## 2. Materials and methods

### 2.1. Plasmids

The plasmid with the coding sequence for rat Cx46 was obtained from Dr. Lisa Ebihara (University of Chicago) (pSP64T-Cx46) [36] and was used for the expression of Cx46 in *Xenopus* oocytes. The mutant Cx46-C3A, which conserves only the extracellular loop Cys residues, was generated *via* site-directed mutagenesis as described elsewhere [37]. In Cx46-C3A, transmembrane Cys 218 and C-terminal domain Cys 283 and 321 were replaced with Ala. The human Cx43, Cx46 and Cx50 cDNAs in the expression plasmid pCMV6-AC-GFP were purchased from OriGene Technologies (Rockville, MD, USA) and used for transfection of HeLa cells. Cx43, Cx46 or Cx50 were fused to TurboGFP, a green fluorescent protein (GFP) variant with improved properties.

### 2.2. Transfection of HeLa cells for Cx43GFP, Cx46GFP and Cx50GFP expression

Parental HeLa cells grown in 35-mm plastic dishes (NunClone) to ~60% confluence were transfected with 1 μg of plasmid (pCMV6-AC-Cx43GFP, pCMV6-AC-Cx46GFP or pCMV6-AC-Cx50GFP) mixed with 4 μg of Lipofectamine 2000 (ThermoFisher, USA). After transfection, the medium was replaced every 2–3 days with DMEM plus 10% SFB supplemented with G418 (Gibco, USA) at 100 μg/ml. G418 was maintained for at least a month to ensure positive selection, and Cx46GFP expression was confirmed by Western blotting and fluorescence microscopy.

### 2.3. cRNA preparation and injection into Xenopus laevis oocytes

SP6-directed capped cRNA synthesis was performed with the mMessage Machine kit (Ambion, Austin, TX) using template plasmids linearized with *Sal I*. Oocytes were injected with 12.5 ng of antisense Cx38 oligonucleotide to reduce Cx38 endogenous expression, in combination with 25 ng of cRNA coding for Cx46 or Cx46-C3A. After cRNA injection, the oocytes were maintained in Barth's solution (in mM: 88 NaCl, 1 KCl, 5 $CaCl_2$, 0.8 $MgCl_2$, and 10 HEPES/NaOH, pH 7.4) supplemented with 0.1 mg/ml gentamycin and 20 units/ml of penicillin and streptomycin for 24–48 h before experimental measurements.

### 2.4. Dye uptake in HeLa cells

The uptake of 4′,6-diamino-2-fenilindol (DAPI; charge −2; MW 277.3) was measured in HeLa cells grown on glass coverslips that were placed in a chamber with 3 ml of recording media (in mM: 140 NaCl, 4 KCl, 5 glucose, and 10 HEPES/NaOH, pH 7.4) plus 10 μM DAPI. Changes in nuclei fluorescence intensity were evaluated from images acquired every 20 s, during a 20-min period, on an inverted microscope (Eclipse Ti-U, Nikon). NIS Elements software (version 4.0, Nikon) was used for data acquisition and off-line image analysis. For the analysis, the fluorescence intensity of at least 16 cells *per* experiment was averaged, and the slope of the increase in fluorescence, which represents the rate of DAPI uptake, was calculated by fitting a linear equation to the data using the GraphPad Prism software version 5. For each measurement, recording solution with 4-HNE was freshly prepared from a 6.5-M stock solution stored at −80 °C.

### 2.5. Xenopus laevis oocytes electrophysiological recordings

Cx46 hemichannel currents were measured in oocytes bathed with ND96 solution (in mM: 96 NaCl, 2 KCl, 1.8 $CaCl_2$, and 5 HEPES/NaOH, pH 7.4) at room temperature. Data acquisition and analysis were performed with pClamp 10/Digidata 1440A A/D Board (Molecular Devices, Foster City, CA). Currents were elicited by 15-s square pulses, ranging from −60 mV to +60 mV in 20 mV steps, from a holding voltage of −60 mV, with 10-s intervals between pulses. Current-voltage (I-V) relationships were calculated from the current values at the end of the pulses.

### 2.6. Cx46 immunoprecipitation

Primary antibodies were attached to magnetic beads following the manufacturer's instructions (Dynabeads antibody coupling kit, ThemoFisher #14311D). Briefly, 1 mg of magnetic beads were mixed with 10 μg of primary antibody and incubated overnight in a roller at 37 °C. Next day the mixture was washed three times with the kit's washing buffer, separating the beads with a small magnet between washes. Then, the anti-Cx46 antibody attached to magnetics beads was resuspended in 100 μl of kit's buffer SB and stored at 4 °C. For the immunoprecipitation studies HeLa Cx46GFP cells were grown in 90-mm plastic dishes (NunClone) to 90% confluence. Cells without treatment or exposed to 100 μM 4-HNE for 20 min at 37 °C were harvested and sonicated in 1 ml PBS with protease inhibitors (cOmplete mini, Roche). Then, 50 μl of mouse anti-Cx46 (Santa Cruz Biotechnology) attached to magnetic beads were added, and the lysate was incubated at 4 °C overnight under constant agitation to avoid agglomeration of the beads. After the incubation, the lysate was placed over a magnet, the supernatant was discarded, and the magnetic beads were washed with 1 ml of PBS. This procedure was repeated three times, and after the final wash the magnetic beads were pelleted with an small magnet, the supernatant was discarded, and 50 μl of PBS plus 100 mM glycine pH 2.0 was added to elute Cx46 from the antibody beads. The mixture was agitated for 1 min, the tube was then placed over the magnet, and the supernatant was placed in a new tube containing 50 μl of 1 M

HEPES/NaOH at pH 7.0 for analysis.

### 2.7. Expression and purification of Cx46

We expressed and purified wild-type human Cx46 followed by a poly-His tag (six His) preceded by a TEV protease cleavage sequence in *E. coli*. XL10-Gold cells (Agilent Technologies, Santa Clara, CA) transformed with Cx46 DNA subcloned into the *NcoI/HindIII* sites of pQE60 (Qiagen, Germantown, MD) were grown at 37 °C in modified M9 minimal medium (180 mM $Na_2HPO_4$, 75 mM $KH_2PO_4$, 30 mM NaCl and 65 mM $NH_4Cl$) supplemented with 10 mM $MgSO_4$, 1% glucose and 0.4 mg/ml ampicillin. The overnight cultures were diluted 25-fold, grown at 37 °C to an $OD_{600}$ ~2, and induced with 0.5 mM isopropyl-β-thiogalactopyranoside for 2 h. Harvesting of the cells and all subsequent procedures were performed at 4 °C unless specified otherwise. The cell pellets were resuspended in buffer A (300 mM NaCl and 50 mM Tris/HCl, pH 8) with 0.5 mM 4-benzenesulfonyl fluoride hydrochloride (Pefabloc), 10 mM $MgCl_2$ and 25 μg/ml DNAse I (Sigma-Aldrich), and lysed on a microfluidizer. Crude membranes were prepared by centrifugation at 100,000 ×*g* for 1 h, followed by solubilization for 4 h with 1% Anzergent 3-12 in 1 M NaCl, 50 mM Tris/HCl, 10% glycerol and 1 mM PMSF, pH 8, at a total protein concentration < 2 mg/ml. The solubilized material, collected after ultracentrifugation at 100,000 ×*g* for 30 min, was loaded onto a Talon $Co^{2+}$ column (Talon Superflow, Clontech) pre-equilibrated with 1 M NaCl, 10% glycerol, 50 mM Tris/NaOH, pH 8, for immobilized metal-affinity chromatography. The resin was washed with 10 column volumes of a solution containing 1 M NaCl, 10% glycerol, 0.05% n-dodecyl-β-D-maltoside, and 50 mM Tris/NaOH, pH 8. After washing with 150 mM NaCl, 10% glycerol, 5 mM imidazole, 0.05% n-dodecyl-β-D-maltoside, and 50 mM Tris/NaOH, pH 8, Cx46 was eluted with a buffer of the same composition, except that imidazole was increased to 300 mM. Fractions containing Cx46 were pooled and the His tag was removed by incubation with TEV protease (1:10 w/w) for 12 h. After removal of the tag, purified Cx46 was isolated by gel filtration chromatography on a Superdex 200 HR column (GE Healthcare) run on an APLC system (LabAlliance, State College, PA).

### 2.8. Western blots analysis

Samples were re-suspended in Laemli's sample buffer, separated on a 10% SDS-PAGE, and electro-transferred to a nitrocellulose membrane using a Dry iBlot Gel Transfer System (Life Technologies). Nonspecific protein binding sites were blocked by incubation of the membrane with 5% nonfat milk/1% Tween-20 TBS buffer (TBS-T) for ~60 min. Membranes were then incubated in blocking buffer containing primary goat anti-HNE (1:100; Cell Biolabs) or mouse anti-Cx46 (1:500; Santa Cruz Biotechnology) antibody. The samples were incubated overnight at 4 °C, followed by five 20-min washes with TBS-T. Then, the membranes were incubated with a secondary antibody conjugated to horseradish peroxidase (1:2000 in 5% nonfat milk/0.1% Tween-20 TBS buffer) and immunoreactivity was detected in a Blot-scanner (CDigit, Licor) for enhanced chemiluminescence using the SuperSignal kit (Pierce, Rockford, IL) according to the manufacturer's instructions.

For Western blot immunoreactive band colocalization, proteins were separated in a 10% SDS-PAGE and then electro-transferred to a PVDF membrane (Immobilion-FL, Merck Millipore) because this membrane has very low autofluorescence in the Odyssey Li-Cor fluorescence image scanner. After the transference, the membrane was blocked as described above, and was then incubated in blocking buffer containing primary goat anti-HNE (1:100; Cell Biolabs) and mouse anti-Cx46 (1:500; Santa Cruz Biotechnology) antibody. The samples were incubated for 48 h at 4 °C, followed by five 20-min washes with blocking buffer. Then, the membranes were incubated for 1 h at room temperature with donkey anti-goat IRDye 680RD and a goat anti-mouse IRDye 800 CW secondary antibodies (Li-Cor) at a dilution of 1:2000 in 5% nonfat milk/0.1% Tween-20 TBS buffer. Fluorescence was detected on a near-infrared scanner (Odyssey, Li-Cor) and colocalized using the scanner's software.

### 2.9. Selenite-induced cataract

Five 10-days-old Sprague-Dawley rats were housed individually in a 12-h light-dark cycle with their mothers and kept in their home cages throughout the study. Sodium selenite (Sigma-Aldrich) was dissolved in sterile saline solution (0.9% NaCl) and administered at 3 mg/kg subcutaneously. Animals from the control group received a single injection of physiological saline solution. After 10 days the rats were anesthetized with 61 mg/kg ketamine, 0.6 mg/kg xylazine and 6.7 mg/kg acepromazine followed by cervical dislocation. Their lenses were extracted and stored in RIPA lysis buffer (Abcam # 156034) with protease inhibitor (cOmplete Mini, # 11836153001. Roche) for Western blot analysis.

### 2.10. Ethical approval

All procedures involving animals were approved by Universidad del Desarrollo and Universidad Andres Bello Bioethical Committees (Acta 030-2015). All procedures were conducted by personal trained to work with animals following local rules for animal care and in accordance to NHI and CONICYT guidelines.

### 2.11. Statistical analysis

Results are expressed as means ± SEM and "n" refers to the number of independent experiments. For statistical analyses and determination of significant differences we used a one-way NOVA or paired Student's *t*-test, as appropriate. Differences were considered significant at $p < 0.05$.

## 3. Results

### 3.1. Functional expression of Cx46 hemichannels in HeLa cells expressing Cx46GFP

HeLa cells were transfected with Cx46GFP and stable clones were selected using G418. Two types of cells were observed after a month of selection: cells with (Fig. 1A, green arrow) and without green fluorescence (Fig. 1A, white arrow). As expected for cells expressing Cx46 hemichannels, the rate of DAPI uptake was higher in the fluorescent cells in divalent cation-free solution (DCFS), a condition that favors hemichannel opening [38] (Fig. 1B). Under control conditions (in presence of extracellular divalent cations), the rate of DAPI uptake was higher in the cells expressing Cx46GFP compared to parental cells (0.30 ± 0.07 AU/s *vs* 0.18 ± 0.05, respectively; Fig. 1C, filled bars), and exposure to DCFS increased the rate in the cells expressing Cx46GFP (to 1.50 ± 0.21 AU/s; Fig. 1C), but had no effect in parental cells (to 0.19 ± 0.02 AU/s; Fig. 1C). Moreover, the rate of DAPI uptake in DCFS was abolished by 200 μM $La^{3+}$ (Fig. 1C; $La^{3+}$), a non-specific hemichannel blocker [34,39]. The results strongly suggest that Cx46GFP forms functional hemichannels in the transfected HeLa cells.

### 3.2. The lipid peroxide 4-HNE reduces Cx46GFP hemichannel activity in HeLa cells

As shown in Fig. 1B–C, there is significant dye uptake in HeLa cells expressing Cx46GFP exposed to DCFS. Fig. 2A (upper panels) shows that after 20-min exposure to 10 μM DAPI in DCFS the nuclei of HeLa cells expressing Cx46GFP acquired blue fluorescence, but in the presence of 100 μM 4-HNE DAPI nuclear fluorescence was drastically reduced (Fig. 2A, lower panels). The inhibition of the DAPI uptake by 4-HNE was concentration dependent, with a 50% inhibition at ~1 μM 4-HNE (52 ± 2%) and 89 ± 4% inhibition at 100 μM 4-HNE (Fig. 2B).

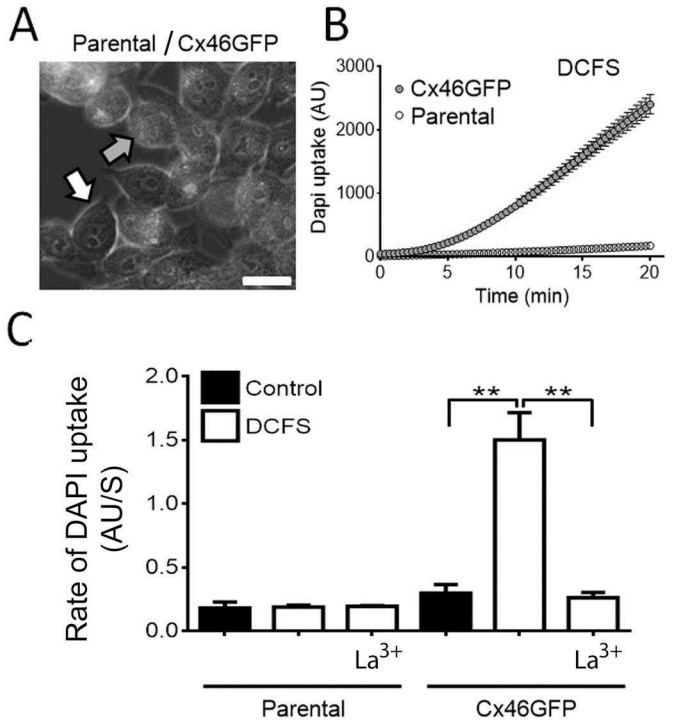


**Fig. 1.** Recombinant hemichannels formed by Cx46GFP in HeLa cells. (A) HeLa cells were stably transfected with a plasmid coding for human Cx46 fused to green fluorescent protein (Cx46GFP). Fluorescent (green arrow) and non-fluorescent cells (white arrow) were identified after selection with G418. Bar = 10 μm. (B) Time course of DAPI uptake (10 μM) in cells exposed to divalent cation-free solution (DCFS). Data are means ± SEM (n = 3, 16 cells *per* measurement). (C) Rate of DAPI uptake (AU/s: arbitrary units/s) in non-fluorescent (parental) cells and cells expressing Cx46GFP. Rates were measured in the presence of divalent cations (control) and in DFCS, with or without 200 μM $La^{3+}$ ($La^{3+}$). See Materials and methods for details. Data are means ± SEM; **denotes p < 0.01.

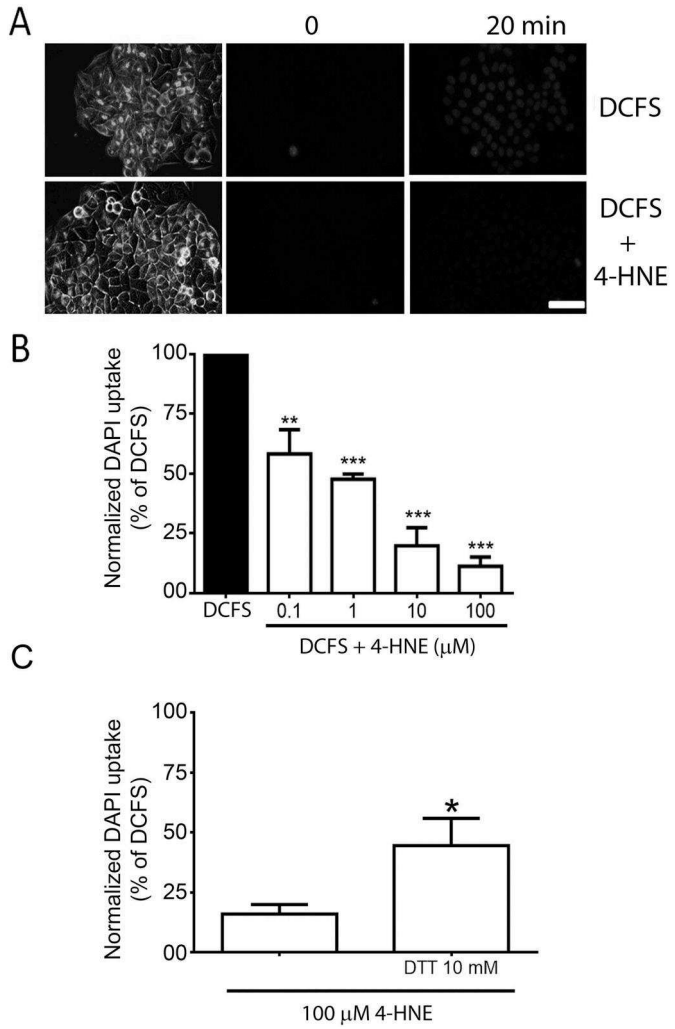


**Fig. 2.** Inhibition of Cx46 hemichannels in HeLa cells by 4-HNE. (A) Images of HeLa cells expressing Cx46GFP exposed to DCFS in the absence (DCFS; top panels) or presence of 100 μM 4-HNE (DCFS + 4-HNE; bottom panels). Left: representative GFP fluorescence images; 0 and 20 min: DAPI fluorescence images acquired at time zero and after 20-min exposure to 10 μM DAPI. Bar = 30 μm. (B) Summary of the rates of DAPI uptake in cells exposed to DCFS in the absence (filled bar) and presence of different concentrations of 4-HNE (open bars). Data are means ± SEM (n = 3, 16 cells *per* measurement); ** denotes p < 0.01 and *** p < 0.001. (C) Effect of DTT on the inhibition of DAPI uptake by 4-HNE. Data from HeLa cells expressing Cx46GFP studied in DCFS after exposure to 100 μM 4-HNE for 15-min, without DTT or followed by exposure to 10 mM DTT. Data were normalized to the rate in DCFS in the absence of drugs (100%) and are presented as means ± SEM (n = 4, 16 cells *per* measurement). The asterisks denote p < 0.05 *vs* DCFS + 100 μM 4-HNE.

To test for the role of Cys oxidation in the effect of 4-HNE, HeLa cells expressing Cx46GFP were first exposed to 100 μM 4-HNE for 10 min, and then to the reducing agent DTT for additional 10 min. The results in Fig. 2C show a partial reversion of the inhibition of DAPI uptake by 10 mM DTT, supporting the notion that oxidation of Cys residues plays a role in the inhibition of Cx46 hemichannels by 4-HNE.

### *3.3. The lipid peroxide 4-HNE induces carbonylation of Cx46GFP*

Cx46GFP from cells HeLa cells without and with exposure to 100 μM 4-HNE (maximal inhibition, Fig. 2B) was immunoprecipitated as described in Materials and Methods, and carbonylation was analyzed by Western blots using an antibody that recognizes protein carbonylation adducts induced by 4-HNE. The anti-4-HNE antibody recognized three major bands immunoprecipitated from cells expressing Cx46GFP that were exposed to 4-HNE. These bands of apparent molecular masses of ~46, 53 and 70 kDa were not present in the absence of exposure to 4-HNE (Fig. 3A). The ~70-kDa band is likely to correspond to Cx46GFP (molecular mass of ~72 kDa), and it is possible that Cx46GFP carbonylation produced the two faster running bands, but we cannot rule out alternative explanations. To confirm Cx46 carbonylation, we performed a similar experiment using Cx46 purified from *E. coli*. While no anti-4-HNE immunoreactive bands were detected in the absence of 4-HNE, exposure to 100 μM 4-HNE yielded a major band at ~46 kDa (Fig. 3B). These results suggest that Cx46 is directly carbonylated upon exposure to 4-HNE. To confirm carbonylation of Cx46 and test for the effect of DTT, we performed experiments in the Odyssey blot scanner, which allowed us to co-localize signals from Cx46 and 4-HNE adducts. The intensity of the bands that reacted with the anti-Cx46 antibody was similar under all conditions (Fig. 3C, Anti-Cx46, and Fig. 3D). In contrast, the intensity of the anti-4-HNE immunoreactive band was weak under control conditions, but increased in presence of 100 μM 4-HNE (Fig. 3C, Anti-4-HNE and Fig. 3E). The merged signals show a co-localization of Cx46 with 4-HNE abducts (Fig. 3C, Merge, fuchsia signal), suggesting that Cx46 is carbonylated by 4-HNE, thus confirming our immunoprecipitation results. In the presence of 10 mM DTT the intensity of the anti-4-HNE immunoreactive bands returned to control values (Fig. 3C and E). From the results presented in this and the preceding section, we propose that Cx46 is carbonylated by 4-HNE and that at least some of the Cx46 Cys residues are the targets.

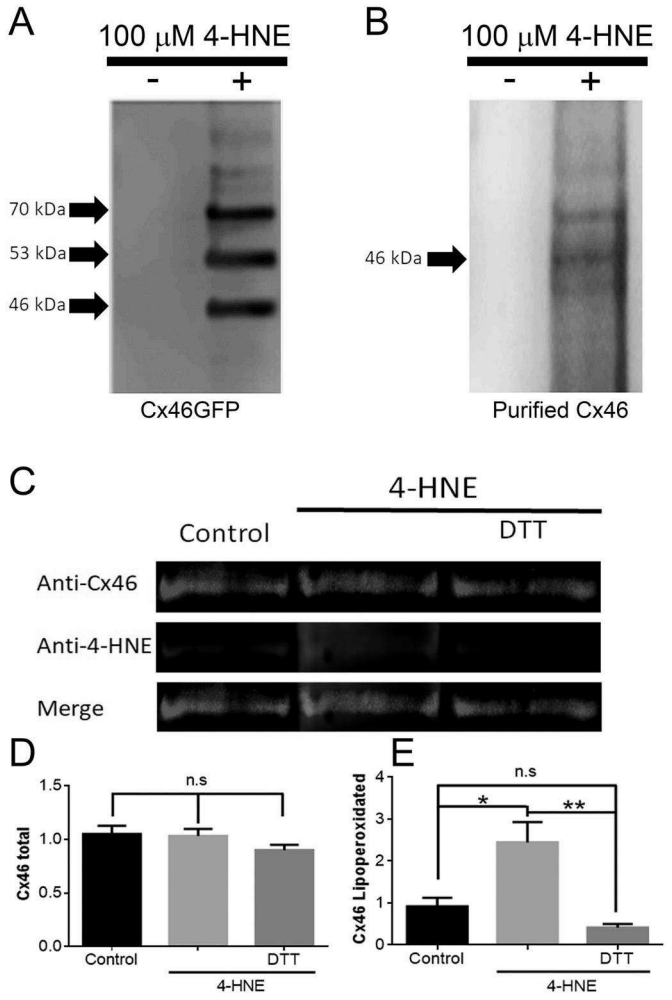


**Fig. 3.** Carbonylation of Cx46 by 4-HNE. (A) Lysates of HeLa cells expressing Cx46GFP under control conditions (−) or exposed to 100 μM 4-HNE for 20 min (+) were immunoprecipitated with an antibody against the C-terminus of Cx46. The immunoprecipitation was then probed for the presence of 4-HNE adducts using an anti-4-HNE antibody. The apparent molecular mass of major immunoreactive bands is indicated by the arrows. The blot is representative of 3 identical experiments. (B) Purified Cx46 under control conditions (−) or treated with 100 μM 4-HNE for 20 min (+) was analyzed for the presence of 4-HNE adducts by Western blotting using the anti-4-HNE antibody described above. The apparent molecular mass of the major immunoreactive band is indicated by the arrow. The blot is representative of 3 identical experiments. (C) Lysates of HeLa cells expressing Cx46GFP under control conditions (left), exposed to 100 μM 4-HNE (middle), or exposed to 100 μM 4-HNE and 10 mM DTT (right). PVDF membranes were incubated with antibodies against Cx46 (red bands) and against 4-HNE (blue bands). Images from fluorescent secondary antibodies were taken in the Odyssey Li-Cor fluorescence image scanner to co-localize both signals (Merge). Plots showing (D) Cx46 and (E) 4-HNE fluorescent intensity quantification under the three experimental conditions. Protein content was normalized by the signal obtained using an antibody against tubulin. Data are means ± SEM (n = 3); * denotes $p < 0.05$ and ** $p < 0.01$.

### 3.4. Intracellular cysteines do not contribute to 4-HNE sensing

The results in Figs. 2C and 3C suggest a role of Cys modification in the effect of 4-HNE. To further test the role of Cx46 Cys, we study the effects of 4-HNE in Cx46 hemichannels expressed in *Xenopus laevis* oocytes using the whole cell voltage clamp technique. Exposure to 100 μM 4-HNE reduced the amplitude of the Cx46 hemichannel currents measured at +60 mV to 57 ± 7% of the initial value (Fig. 4A, upper recordings). Then, we evaluated the inhibition by 4-HNE of hemichannels formed by a Cx46 mutant that retains only the native Cys

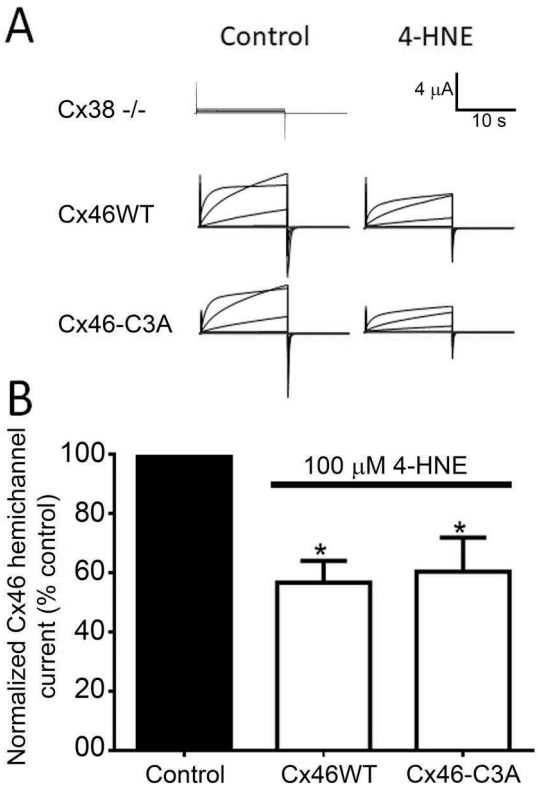


**Fig. 4.** Cx43 hemichannels lacking intracellular Cys are inhibited by 4-HNE. (A) Representative hemichannel currents from *Xenopus* oocytes injected only with an oligo anti-Cx38 (Cx38 −/−) or expressing wild-type Cx46 (Cx46WT) or a Cx46 mutant that retains only the six extracellular Cys (Cx46-C3A). Recordings were obtained in DCFS (n = 7) and DCFS with 4-HNE (100 μM for 5 min; n = 7). (B) Summary of the effects of 4-HNE on the hemichannel currents measured at +60 mV. The currents were normalized to the DCFS value in the absence of 4-HNE (control). Data are means ± SEM and the asterisk denote $p < 0.05$ *vs* control.

residues in the extracellular loops (Cx46-C3A). The control Cx46-C3A hemichannel current was similar to that of hemichannels formed by wild-type Cx46 (Cx46WT; Fig. 4A). Interestingly, after exposure to 100 μM 4-HNE, the decrease in Cx46-C3A hemichannel current was indistinguishable from that of Cx46WT hemichannels (Fig. 4B). These results demonstrate that the intracellular (Cys283 and Cys321) and the TM4 Cys (Cys218) are not involved in the inhibition of Cx46 hemichannels by 4-HNE, and point to one or more of the six extracellular Cys as the 4-HNE sensor(s). Unfortunately, mutants in which extracellular Cys were replaced with Ala did not form functional hemichannels (data not shown) and we were not able to further test directly the role of these Cys in the inhibition by 4-HNE.

### 3.5. Cx46 is carbonylated in an animal model of cataract

Cx46 is mostly expressed in fiber cells of the lens [40] and in humans and animal models mutations in its gene (GJA3) are associated with cataract formation [40]. In a previous studies, we found that Cx46 was S-nitrosylated in an animal model of selenite-induced cataract [26]. Suggesting that post-translational modifications of Cx46 are associated to ROS/RNS production. To test the hypothesis that Cx46 could be affected by 4-HNE *in vivo*, we evaluated whether Cx46 is carbonylated in a selenite-induced cataract model [42,43]. Consistent with our previous work [41], under control conditions the lenses were transparent (Fig. 5A, left panel), whereas in rats injected with selenite the lenses presented extensive cataracts (Fig. 5A, right panel). Western blot analysis showed a red band of ~46-kDa in lenses from control rats (Fig. 5B,

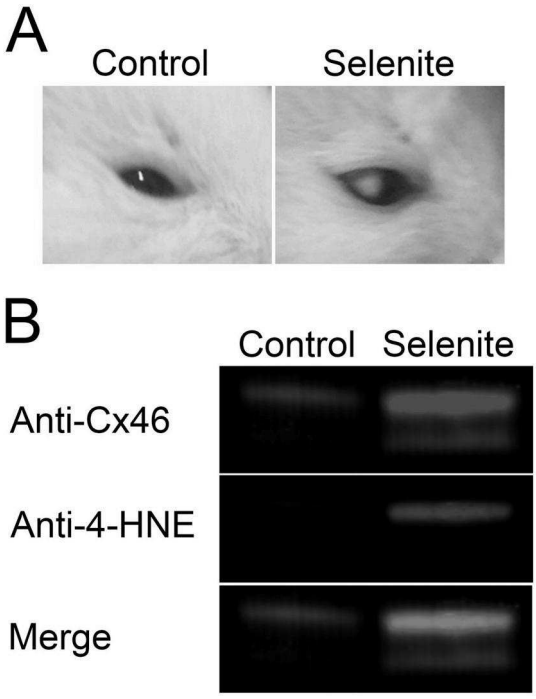


**Fig. 5.** Cx46 carbonylation is associated with cataracts in an animal model. Lenses from Sprague-Dawley rats were extracted 10 days after receiving a single subcutaneous injection of sodium selenite (3 mg/kg) or vehicle (saline solution 0.9% NaCl). (A) Representative images of lenses from rats under control conditions (left) or injected with sodium selenite (right) (n = 5 animals *per* condition). (B) Samples from animals shown above were analyzed by Western blotting to assess colocalization of signals from specific antibodies against Cx46 (red) and 4-HNE abducts (blue).

Anti-Cx46), whereas in lenses from selenite-treated animals there was an evident increase in Cx46, and especially carbonylated Cx46 (Fig. 5B, Merge). These results demonstrate that Cx46 is post-translationally modified by 4-HNE in lenses with cataracts induced by selenite.

### *3.6. Hemichannels formed by Cx43, but not those formed by Cx50, are inhibited by 4-HNE*

Equatorial cells of the human lens express Cx43 and Cx50, whereas mature fiber cells located at the lens nucleus express Cx46 and Cx50 [44]. The results above showed that treatment with 4-HNE inhibited Cx46 hemichannels. Here, we tested whether 4-HNE also affects hemichannels formed the other lens connexins. The rate of DAPI uptake of HeLa cells expressing Cx43GFP (Fig. 6A) increased from 0.38 ± 0.02 (AU/s) (Fig. 6C) under control conditions to 1.07 ± 0.07 (AU/s) in DCFS, an effect that was reduced to 0.62 ± 0.05 (AU/s) by exposure to 100 μM of 4-HNE (Fig. 6C). The effect of 4-HNE on Cx43 hemichannels (65% inhibition) was smaller than that observed in Cx46 hemichannels (89%). Contrary to Cx43 and Cx46 hemichannels, Cx50 hemichannels expressed in HeLa cells (Fig. 6B) were not affected by 4-HNE (Fig. 6D). The rate of dye uptake in DCFS was not affected by 100 mM 4-HNE, with values of 0.58 ± 0.06 and 0.63 ± 0.07 (AU/s) before and after 4-HNE treatment, respectively. These data suggest that 4-HNE affects Cx46 > Cx43, and does not affect Cx50 hemichannels.

## 4. Discussion

In this work we demonstrate that the lipid peroxide 4-HNE inhibits recombinant Cx46 hemichannels expressed in HeLa cells and *Xenopus laevis* oocytes. This effect was associated with Cx46 carbonylation, suggesting a direct regulatory role of the lipid peroxide on Cx46 hemichannels. The anti-4-HNE antibody that we used to assess Cx46

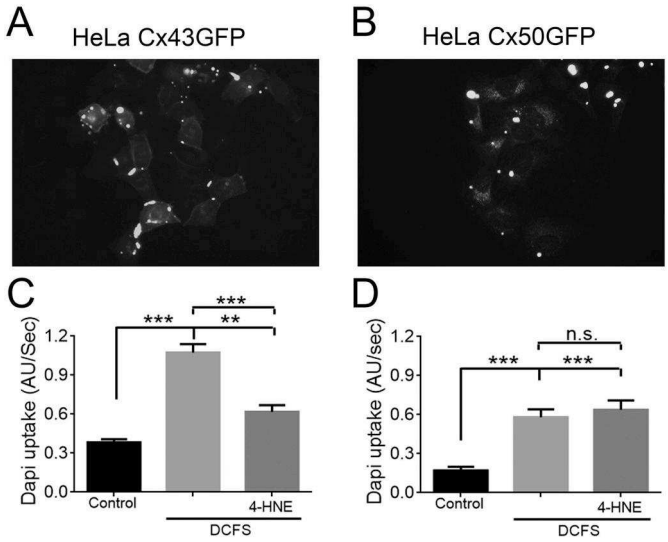


**Fig. 6.** 4-HNE inhibits of hemichannels formed by Cx43, but not those formed by Cx50. (A) Images of HeLa cells expressing Cx43GFP or (B) Cx50GFP. Summary of the rates of DAPI uptake in (C) HeLa Cx43GFP and (D) HeLa Cx50GFP cells under control conditions (filled bar), exposed to DCFS (light grey) or exposed to DCFS plus 100 μM 4-HNE (darker grey). Data are means ± SEM (n = 4, at least 12 cells *per* measurement); ** denotes $p < 0.01$ and *** $p < 0.001$.

carbonylation does not distinguish between carbonylated amino acids. However, carbonylation by 4-HNE shows a strong preference for Cys > His > Lys [15], and the inhibition of Cx46 hemichannels by 4-HNE and their carbonylation was partially reversed by the Cys-reducing agent DTT. These observations point to a critical role of Cys carbonylation in the response of Cx46 hemichannels to 4-HNE. Furthermore, the inhibition by 4-HNE was intact in hemichannels formed by a Cx46 mutant in which only the native extracellular Cys were present. From these results, we conclude that 4-HNE is a novel Cx46 hemichannel regulator, and that its effect is due, at least in part, to carbonylation of one or more of the Cys in the extracellular loops. Considering that these Cys are not accessible for modification in GJCs, the role of extracellular loop Cys is consistent with the selective effect of linoleic acid, which affects hemichannels, but not GJCs [31].

In a previous work, we demonstrated that some PUFAs inhibit Cx46 hemichannels, and that the effects of linoleic acid appear to be direct on Cx46 [31]. Since linoleic acid is a precursor of the lipid peroxide 4-HNE, it is possible that this PUFA inhibits Cx46 hemichannels through its oxidized form. Here, we demonstrate that 4-HNE is a potent Cx46 hemichannel blocker, so the effects of linoleic acid or any other PUFAs on hemichannel activity should be revised to consider the possibility that they result from the effects of lipid peroxides in general, and 4-HNE in particular.

Protein carbonylation is known as a marker of oxidative stress and is linked to various human diseases [45], Protein carbonylation is an oxidative posttranslational modification that can principally be induced by lipid peroxides, such as 4-HNE, metal-induced oxidation and reducing sugars or dicarbonyl compounds derived from the sugars (such as glyoxal, methylglyoxal and 3-deoxyglucosone) [45,46]. The source of protein carbonylation that mediates Cx46 oxidation in the lens is a matter for future studies, but as suggested by Fedorova and co-workers [45], it could depend on specific oxidative conditions and could be correlated with specific diseases [45]. Additionally, it could depend on the sequence of particular proteins because it is known that the S-nitrosylation of a specific Cys depends on the amino acids close to it [47] and not all Cys are affected by nitric oxide in a protein [48].

Lens cells can release and take-up GSH as a scavenger of toxic molecules such as oxygen reactive molecules [49,50]. They also release

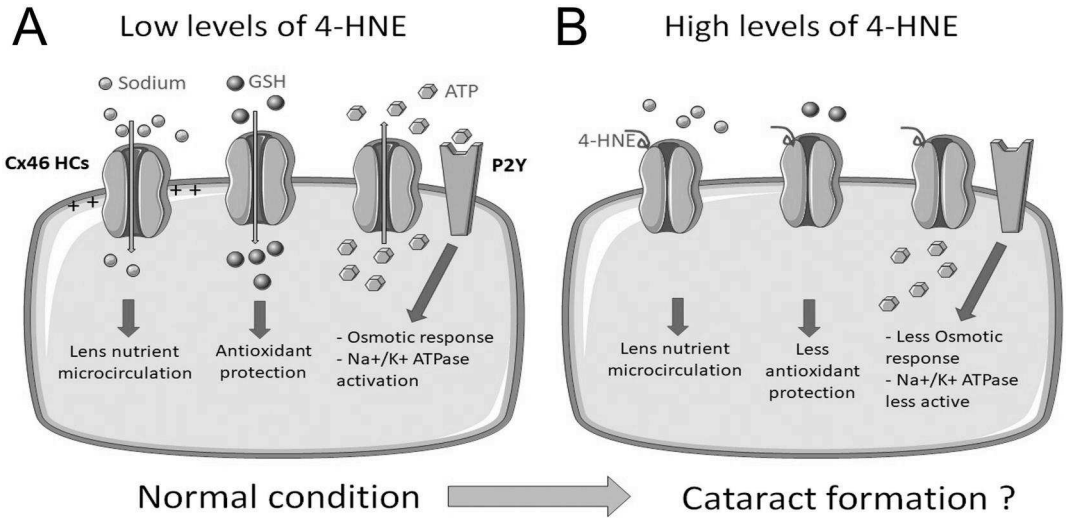


**Fig. 7.** Model explaining a potential mechanism of cataract formation in response to hemichannel inhibition. (A) Under control conditions in which 4-HNE levels are low and hemichannels have a "normal" open probability that is sufficient to allow uptake and/or release of $Na^+$, GSH and ATP. These mediators participate in important cellular processes in the lens. (B) When inflammatory conditions are set (*e.g.* diabetes, aging) an increase of 4-HNE levels is expected and hemichannel activity will be lower, resulting in reduced fluxes of $Na^+$, GSH and ATP. This will alter lens micronutrient circulation, antioxidant protection, osmotic response and $Na^+/K^+$ ATPase activity, which could participate in cataract formation.

ATP, which through the activation of purinergic receptors can activate Src kinase and increase $Na^+$-$K^+$-ATPase activity [51]. Moreover, $Na^+$ fluxes are fundamental for the microcirculation of nutrients and therefore lens transparency [50]. Hemichannels formed by Cx43 or Cx46 are permeable to GSH [52], $Na^+$ [53], and ATP [54,55]. Based on our results, 4-HNE in lens cells could carbonylate Cx46 (and probably Cx43) hemichannels and decrease their activity (Fig. 7). As a consequence of hemichannel inhibition, less $Na^+$, GSH and ATP will be released, which in turn will decrease nutrient microcirculation, antioxidant protection and osmotic response (Fig. 7). In support of this notion, high levels of 4-HNE in lens and blood serum are well correlated with cataract formation [56–58].

## 5. Conclusion

In this work we present data supporting the hypothesis that carbonylation of Cx46 extracellular Cys by the lipid peroxide 4-HNE inhibits Cx46 hemichannels, an effect that may promote cataract formation in the eye lens.

## Declaration of competing interest

The authors of this work declare no competing interest.

## Acknowledgments

This work was supported by the Fondo Nacional de Desarrollo Científico y Tecnológico (FONDECYT) No. 1160227 (MR), No. 1160986 (JS) and No. 1200452 (JS).

## References

[1] M.A. Retamal, E.P. Reyes, I.E. García, B. Pinto, A.D. Martínez, C. González, Diseases associated with leaky hemichannels, Front. Cell. Neurosci. 9 (2015), https://doi.org/10.3389/fncel.2015.00267.
[2] J.C. Sáez, V.M. Berthoud, M.C. Brañes, A.D. Martínez, E.C. Beyer, Plasma membrane channels formed by connexins: their regulation and functions, Physiol. Rev. 83 (2003) 1359–1400, https://doi.org/10.1152/physrev.00007.2003.
[3] J.-C. Hervé, M. Derangeon, Gap-junction-mediated cell-to-cell communication, Cell Tissue Res. 352 (2013) 21–31, https://doi.org/10.1007/s00441-012-1485-6.
[4] J.E. Contreras, J.C. Saez, F.F. Bukauskas, M.V.L. Bennett, Gating and regulation of connexin 43 (Cx43) hemichannels, Proc. Natl. Acad. Sci. 100 (2003) 11388–11393, https://doi.org/10.1073/pnas.1434298100.
[5] J.A. Orellana, M.A. Retamal, R. Moraga-Amaro, J. Stehberg, Role of astroglial hemichannels and pannexons in memory and neurodegenerative diseases, Front. Integr. Neurosci. 10 (2016), https://doi.org/10.3389/fnint.2016.00026.
[6] V. Abudara, M.A. Retamal, R. Del Rio, J.A. Orellana, Synaptic Functions of Hemichannels and Pannexons: A Double-Edged Sword, Front Mol Neurosci 11 (2018) 435, https://doi.org/10.3389/fnmol.2018.00435.
[7] Z.-C. Ye, M.S. Wyeth, S. Baltan-Tekkok, B.R. Ransom, Functional hemichannels in astrocytes: a novel mechanism of glutamate release, J. Neurosci. 23 (2003) 3588–3596.
[8] J. Stehberg, R. Moraga-Amaro, C. Salazar, A. Becerra, C. Echeverría, J.A. Orellana, G. Bultynck, R. Ponsaerts, L. Leybaert, F. Simon, J.C. Sáez, M.A. Retamal, Release of gliotransmitters through astroglial connexin 43 hemichannels is necessary for fear memory consolidation in the basolateral amygdala, FASEB J. 26 (2012) 3649–3657, https://doi.org/10.1096/fj.11-198416.
[9] J.C. Sáez, S. Contreras-Duarte, G.I. Gómez, V.C. Labra, C.A. Santibañez, R. Gajardo-Gómez, B.C. Avendaño, E.F. Díaz, T.D. Montero, V. Velarde, J.A. Orellana, Connexin 43 hemichannel activity promoted by pro-inflammatory cytokines and high glucose alters endothelial cell function, Front. Immunol. 9 (2018) 1899, https://doi.org/10.3389/fimmu.2018.01899.
[10] B.C. Stong, Q. Chang, S. Ahmad, X. Lin, A novel mechanism for connexin 26 mutation linked deafness: cell death caused by leaky gap junction hemichannels, Laryngoscope. 116 (2006) 2205–2210, https://doi.org/10.1097/01.mlg.0000241944.77192.d2.
[11] G.S.L. Liang, M. de Miguel, J.M. Gómez-Hernández, J.D. Glass, S.S. Scherer, M. Mintz, L.C. Barrio, K.H. Fischbeck, Severe neuropathy with leaky connexin32 hemichannels, Ann. Neurol. 57 (2005) 749–754, https://doi.org/10.1002/ana.20459.
[12] Y. Niwa, Lipid peroxides and superoxide dismutase (SOD) induction in skin inflammatory diseases, and treatment with SOD preparations, Dermatologica. 179 (Suppl. 1) (1989) 101–106.
[13] F. Ito, Y. Sono, T. Ito, Measurement and clinical significance of lipid peroxidation as a biomarker of oxidative stress: oxidative stress in diabetes, atherosclerosis, and chronic inflammation, Antioxidants 8 (2019), https://doi.org/10.3390/antiox8030072.
[14] A. Ayala, M.F. Muñoz, S. Argüelles, Lipid peroxidation: production, metabolism, and signaling mechanisms of malondialdehyde and 4-hydroxy-2-nonenal, Oxidative Med. Cell. Longev. 2014 (2014) 360438, https://doi.org/10.1155/2014/360438.
[15] H. Zhang, H.J. Forman, Signaling by 4-hydroxy-2-nonenal: exposure protocols, target selectivity and degradation, Arch. Biochem. Biophys. 617 (2017) 145–154, https://doi.org/10.1016/j.abb.2016.11.003.
[16] E. Niki, Lipid peroxidation: physiological levels and dual biological effects, Free Radic. Biol. Med. 47 (2009) 469–484, https://doi.org/10.1016/j.freeradbiomed.2009.05.032.
[17] R.J. Schaur, W. Siems, N. Bresgen, P.M. Eckl, 4-Hydroxy-nonenal-a bioactive lipid peroxidation product, Biomolecules. 5 (2015) 2247–2337, https://doi.org/10.3390/biom5042247.
[18] M.M. Gaschler, B.R. Stockwell, Lipid peroxidation in cell death, Biochem. Biophys. Res. Commun. 482 (2017) 419–425, https://doi.org/10.1016/j.bbrc.2016.10.086.
[19] J.P. Castro, T. Jung, T. Grune, W. Siems, 4-Hydroxynonenal (HNE) modified proteins in metabolic diseases, Free Radic. Biol. Med. 111 (2017) 309–315, https://doi.org/10.1016/j.freeradbiomed.2016.10.497.
[20] T. Ruskovska, D.A. Bernlohr, Oxidative stress and protein carbonylation in adipose tissue - implications for insulin resistance and diabetes mellitus, J. Proteome 92

(2013) 323–334, https://doi.org/10.1016/j.jprot.2013.04.002.
[21] A. Higdon, A.R. Diers, J.Y. Oh, A. Landar, V.M. Darley-Usmar, Cell signalling by reactive lipid species: new concepts and molecular mechanisms, Biochem. J. 442 (2012) 453–464, https://doi.org/10.1042/BJ20111752.
[22] Y.S. Kim, Z.Y. Park, S.Y. Kim, E. Jeong, J.Y. Lee, Alteration of Toll-like receptor 4 activation by 4-hydroxy-2-nonenal mediated by the suppression of receptor homodimerization, Chem. Biol. Interact. 182 (2009) 59–66, https://doi.org/10.1016/j.cbi.2009.07.009.
[23] Q. Chen, T.W. Jones, P.C. Brown, J.L. Stevens, The mechanism of cysteine conjugate cytotoxicity in renal epithelial cells. Covalent binding leads to thiol depletion and lipid peroxidation, J. Biol. Chem. 265 (1990) 21603–21611.
[24] C.-M. Wong, L. Marcocci, D. Das, X. Wang, H. Luo, M. Zungu-Edmondson, Y.J. Suzuki, Mechanism of protein decarbonylation, Free Radic. Biol. Med. 65 (2013) 1126–1133, https://doi.org/10.1016/j.freeradbiomed.2013.09.005.
[25] D.L. Carbone, J.A. Doorn, Z. Kiebler, D.R. Petersen, Cysteine modification by lipid peroxidation products inhibits protein disulfide isomerase, Chem. Res. Toxicol. 18 (2005) 1324–1331, https://doi.org/10.1021/tx050078z.
[26] M.V. Bennett, J.M. Garré, J.A. Orellana, F.F. Bukauskas, M. Nedergaard, J.C. Sáez, Connexin and pannexin hemichannels in inflammatory responses of glia and neurons, Brain Res 1487 (2012) 3–15, https://doi.org/10.1016/j.brainres.2012.08.042.
[27] P.J. Sáez, K.F. Shoji, A. Aguirre, J.C. Sáez, Regulation of hemichannels and gap junction channels by cytokines in antigen-presenting cells, Mediators Inflamm 2014 (2014) 742734, https://doi.org/10.1523/1155/2014/742734.
[28] J.A. Orellana, A.D. Martinez, M.A. Retamal, Gap junction channels and hemichannels in the CNS: regulation by signaling molecules, Neuropharmacology 75 (2013), https://doi.org/10.1016/j.neuropharm.2013.02.020.
[29] J. Willebrords, S. Crespo Yanguas, M. Maes, E. Decrock, N. Wang, L. Leybaert, B.R. Kwak, C.R. Green, B. Cogliati, M. Vinken, Connexins and their channels in inflammation, Crit. Rev. Biochem. Mol. Biol. 51 (2016) 413–439, https://doi.org/10.1080/10409238.2016.1204980.
[30] C. Puebla, M.A. Retamal, R. Acuña, J.C. Sáez, Regulation of connexin-based channels by fatty acids, Front. Physiol. 8 (2017) 11, https://doi.org/10.3389/fphys.2017.00011.
[31] M.A. Retamal, F. Evangelista-Martínez, C.G. León-Paravic, G.A. Altenberg, L. Reuss, Biphasic effect of linoleic acid on connexin 46 hemichannels, Pflugers Arch. Eur. J. Physiol. 461 (2011), https://doi.org/10.1007/s00424-011-0936-3.
[32] D.-P. Wu, T.-Y. Lin, L.-R. Bai, J.-L. Huang, Y. Zhou, N. Zhou, S.-L. Zhong, S. Gao, X.-X. Yin, Enhanced phototoxicity of photodynamic treatment by Cx26-composed GJIC via ROS-, calcium- and lipid peroxide-mediated pathways, J. Biophotonics 10 (2017) 1586–1596, https://doi.org/10.1002/jbio.201600255.
[33] T. Yamaguchi, M. Yoneyama, E. Hinoi, K. Ogita, Involvement of calpain in 4-hydroxynonenal-induced disruption of gap junction-mediated intercellular communication among fibrocytes in primary cultures derived from the cochlear spiral ligament, J. Pharmacol. Sci. 129 (2015) 127–134, https://doi.org/10.1016/j.jphs.2015.09.005.
[34] M.A. Retamal, N. Froger, N. Palacios-Prado, P. Ezan, P.J. Saez, J.C. Saez, C. Giaume, Cx43 hemichannels and gap junction channels in astrocytes are regulated oppositely by proinflammatory cytokines released from activated microglia, J. Neurosci. 27 (2007) 13781–13792, https://doi.org/10.1523/JNEUROSCI.2042-07.2007.
[35] M.A. Retamal, Carbon monoxide modulates connexin function through a lipid peroxidation-dependent process: a hypothesis, Front. Physiol. 7 (2016) 259, https://doi.org/10.3389/fphys.2016.00259.
[36] D.L. Paul, L. Ebihara, L.J. Takemoto, K.I. Swenson, D.A. Goodenough, Connexin46, a novel lens gap junction protein, induces voltage-gated currents in nonjunctional plasma membrane of Xenopus oocytes, J. Cell Biol. 115 (1991) 1077–1089.
[37] M.A. Retamal, S. Yin, G.A. Altenberg, L. Reuss, Modulation of Cx46 hemichannels by nitric oxide, Am. J. Physiol. Physiol. 296 (2009) C1356–C1363, https://doi.org/10.1152/ajpcell.00054.2009.
[38] W. Lopez, J. Ramachandran, A. Alsamarah, Y. Luo, A.L. Harris, J.E. Contreras, Mechanism of gating by calcium in connexin hemichannels, Proc. Natl. Acad. Sci. 113 (2016) E7986–E7995, https://doi.org/10.1073/pnas.1609378113.
[39] R.P. Kondo, S.-Y. Wang, S.A. John, J.N. Weiss, J.I. Goldhaber, Metabolic inhibition activates a non-selective current through connexin hemichannels in isolated ventricular myocytes, J. Mol. Cell. Cardiol. 32 (2000) 1859–1872, https://doi.org/10.1006/jmcc.2000.1220.
[40] V.M. Berthoud, A. Ngezahayo, Focus on lens connexins, BMC Cell Biol. 18 (2017) 6, https://doi.org/10.1186/s12860-016-0116-6.
[41] M.A. Retamal, V.P. Orellana, N.J. Arévalo, C.G. Rojas, R.J. Arjona, C.A. Alcaíno, W. González, J.G. Canan, R. Moraga-Amaro, J. Stehberg, L. Reuss, G.A. Altenberg, Cx46 hemichannel modulation by nitric oxide: role of the fourth transmembrane helix cysteine and its possible involvement in cataract formation, Nitric Oxide 86 (2019) 54–62, https://doi.org/10.1016/j.niox.2019.02.007.
[42] N.J. Russell, J.E. Royland, E.L. McCawley, T.R. Shearer, Ultrastructural study of selenite-induced nuclear cataracts, Invest. Ophthalmol. Vis. Sci. 25 (1984) 751–757.
[43] P.J. Avarachan, U.M. Rawal, Protein profile in the progressive experimental cataract (selenite model)., Indian J. Ophthalmol. 33 (n.d.) 303–8.
[44] E.C. Beyer, V.M. Berthoud, Connexin hemichannels in the lens, Front. Physiol. 5 (2014) 20, https://doi.org/10.3389/fphys.2014.00020.
[45] M. Fedorova, R.C. Bollineni, R. Hoffmann, Protein carbonylation as a major hallmark of oxidative damage: update of analytical strategies, Mass Spectrom. Rev. 33 (2014) 79–97, https://doi.org/10.1002/mas.21381.
[46] E.R. Stadtman, R.L. Levine, Protein oxidation, Ann. N. Y. Acad. Sci. 899 (2006) 191–208, https://doi.org/10.1111/j.1749-6632.2000.tb06187.x.
[47] J. Hu, X. Huang, L. Chen, X. Sun, C. Lu, L. Zhang, Y. Wang, J. Zuo, Site-specific nitrosoproteomic identification of endogenously S-nitrosylated proteins in Arabidopsis, Plant Physiol. 167 (2015) 1731–1746, https://doi.org/10.1104/pp.15.00026.
[48] I. Kovacs, C. Lindermayr, Nitric oxide-based protein modification: formation and site-specificity of protein S-nitrosylation, Front. Plant Sci. 4 (2013), https://doi.org/10.3389/fpls.2013.00137.
[49] M.F. Lou, Redox regulation in the lens, Prog. Retin. Eye Res. 22 (2003) 657–682.
[50] J.C. Lim, A. Umapathy, A.C. Grey, E. Vaghefi, P.J. Donaldson, Novel roles for the lens in preserving overall ocular health, Exp. Eye Res. 156 (2017) 117–123, https://doi.org/10.1016/j.exer.2016.05.027.
[51] M. Shahidullah, A. Mandal, C. Beimgraben, N.A. Delamere, Hyposmotic stress causes ATP release and stimulates Na, K-ATPase activity in porcine lens, J. Cell. Physiol. 227 (2012) 1428–1437, https://doi.org/10.1002/jcp.22858.
[52] X. Tong, W. Lopez, J. Ramachandran, W.A. Ayad, Y. Liu, A. Lopez-Rodriguez, A.L. Harris, J.E. Contreras, Glutathione release through connexin hemichannels: implications for chemical modification of pores permeable to large molecules, J. Gen. Physiol. 146 (2015) 245–254, https://doi.org/10.1085/jgp.201511375.
[53] L. Ebihara, Y. Korzyukov, S. Kothari, J.-J. Tong, Cx46 hemichannels contribute to the sodium leak conductance in lens fiber cells, Am. J. Physiol. Physiol. 306 (2014) C506–C513, https://doi.org/10.1152/ajpcell.00353.2013.
[54] C.E. Stout, J.L. Costantin, C.C.G. Naus, A.C. Charles, Intercellular calcium signaling in astrocytes via ATP release through connexin hemichannels, J. Biol. Chem. 277 (2002) 10482–10488, https://doi.org/10.1074/jbc.M109902200.
[55] M.L. Cotrina, J.H.C. Lin, J.C. López-García, C.C.G. Naus, M. Nedergaard, ATP-mediated glia signaling, J. Neurosci. 20 (2000) 2835–2844, https://doi.org/10.1523/jneurosci.20-08-02835.2000.
[56] D. Chang, X. Zhang, S. Rong, Q. Sha, P. Liu, T. Han, H. Pan, Serum antioxidative enzymes levels and oxidative stress products in age-related cataract patients, Oxidative Med. Cell. Longev. 2013 (2013) 1–7, https://doi.org/10.1155/2013/587826.
[57] N.H. Ansari, L. Wang, S.K. Srivastava, Role of lipid aldehydes in cataractogenesis: 4-hydroxynonenal-induced cataract, Biochem. Mol. Med. 58 (1996) 25–30.
[58] S.K. Srivastata, S. Awasthi, L. Wang, A. Bhatnagar, Y.C. Awasthi, N.H. Ansari, Attenuation of 4-hydroxynonenal-induced cataractogenesis in rat lens by butylated hydroxytoluene, Curr. Eye Res. 15 (1996) 749–754.